Biochimica et Biophysica Acta, 640 (1981) 142—158

BBA 79034

EVALUATION OF THE ELECTRON DENSITY PROFILE OF THE FROG ROD OUTER SEGMENT DISC-MEMBRANE IN VIVO USING X-RAY DIFFRACTION *

J. FUNK, W. WELTE, N. HODAPP, I. WUTSCHEL and W. KREUTZ

Institut für Biophysik und Strahlenbiologie der Universität Freiburg im Breigau, Albertstrasse 23, D-7800 Freiburg im Breisgau (F.R.G.)

(Received April 29th, 1980)

Key words: Electron density profile; Rod outer segment; X-ray diffraction pattern; Rhodopsin

Summary

The structure of the rod outer segment disc-membrane in vivo was studied by X-ray low-angle scattering. The experiments were made on frogs under narcosis.

Diffraction patterns corresponding to a resolution of 1.5 nm could be obtained from the membrane stacks of the rod outer segment discs.

For the analysis of the measured diffraction pattern a new special computer procedure was elaborated. Among other generalizations of the theory, it was taken into account that the electron densities in the inter- and intra-disc spaces differ from the mean electron density of the whole stack. The consideration of this possibility, together with an exact experimental measurement of the isotrope background scattering, led to a mathematically unique solution.

The calculated electron density profile apparently is a distinct asymmetric bilayer. The electron density on the side of the membrane which is in contact with the disc lumen is higher than the electron density on the side in contact with the cytoplasm. Therefore, a localization of rhodopsin or of other high molecular proteins mainly on the cytoplasmatic edge of the membrane can be excluded for the rod outer segment discs in vivo.

Introduction

The rod outer segments of the vertebrate retina are composed of about 2000 regularly stacked, closed and flattened vesicles. The special significance of these membrane vesicles, called discs, lies in the fact that the primary process of visual perception takes place in these discs. The primary process is initiated by

* An abstract of this paper was published in 'Annual Meeting of the German Biophysics Society' (1979) [14].

the absorption of the incident photon by rhodopsin, a special protein of the disc membrane. After that, rhodopsin dissociates, through a number of intermediate stages, into a protein, the so-called opsin, and into a chromophore, the so-called all-*trans*-retinal. Details on secondary reactions, producing a depolarisation of the exterior cell membrane, are as yet not clearly known. Kinetic light-scattering experiments [1,2], however, indicate that changes of the membrane structure of the disc play an important role in these secondary reactions.

Therefore, more detailed information than hitherto available on the structure of the rod outer segment disc membrane, especially under in vivo conditions, is necessary to really understand this part of the visual perception.

Because of the quasi-crystalline stacking of the discs the X-ray low-angle scattering offers a suitable method for the required structure investigations. Even though structure investigations by X-ray low-angle scattering have been published for more than ten years [3—5] the electron density profile of the disc membrane is still disputed in literature. The published electron density profiles show agreement only in the following points: 1, The stacking period ('Bragg period') of the discs amounts to about 30 nm. 2, The basis structure of the disc membrane is a lipid bilayer. 3, The extension of a disc in the direction of the stacking axis is about 15—18 nm.

Regarding further important details on the profile, there exist various and even partly contradictory results up to now. For example, profiles which show a higher electron density on the cytoplasmatic side of the membrane than on the side which is in contact with the disc lumen were calculated [6,7] in the same way as profiles with an opposite asymmetry [8,9] (for further details see Discussion).

A possible reason for the disagreement among the published profiles is that probably in each case the significance of an exact measurement of the isotrope background scattering may have been underestimated.

Moreover, even the best of the evaluation methods developed hitherto [8] are not generally valid enough to allow a unique determination. Therefore, additional and unproven assumptions about the disc membrane were still used in these methods, as, for instance, the hypothesis that the electron density in the disc lumen and in the cytoplasm is identical to the mean electron density of the whole membrane stack.

Furthermore, compared with other methods of structure research, for example light scattering or electron microscopy, a major advantage of the X-ray structure analysis is the possibility of studying specimens in vivo. Nevertheless, up to now it has been possible in only one study [10,11] to obtain X-ray diffraction-patterns of the rod outer segments in vivo; in this case, however, the achieved experimental data did not suffice to allow a determination of the electron density profile [12]. The prompting to apply the X-ray method again, was therefore suggested by the facts: (a) that a generalized evaluation theory has been developed [13] which allows the determination of a mathematically unique solution without any unproved additional assumption and (b) that experimental methods were elaborated which allowed the achievement of diffraction patterns with a high resolution and sufficiently small statistical noise as well as the measurement of the background scattering.

Material and Methods

Experiments were made on two different species of frog *Rana temporaria* (body length, 3—5 cm) and *Rana esculenta* (body length, 6—8 cm). A difference in the quality of the diffraction-patterns of both species was not detected within the limits of the measuring accuracy.

The animals were narcotized by an aqueous solution of the anaesthetic 'MS 222' ('Methansulfonat des Meta-Amino-Benzoesäure-Aetylesters', Sandoz AG., Basel), concentration, 0.5 g/l. Also, throughout the measurement, the animals, which were placed into a specially constructed 'specimen-holder', were washed all around by this anaesthetic solution. In this way, the required moistening of the frogs' skin was simultaneously ensured. 'Specimen-holder' and anaesthetic solution were cooled down to 1°C. It was found that this precondition was necessary to obtain an adequate diffraction pattern. All experiments were carried out under neon light. Proof of the living state of the frogs was given by the fact that half an hour after each experiment the animals showed quite normal reflexes.

Specimen preparation

The preparation of the eye will be described at greater detail, this being a key-factor for achieving satisfactory experimental results.

It is not possible to obtain diffraction patterns of the rod outer segments of a living frog without dissecting the skin covering the eye and the sclera from the site of irradiation. It is relatively simple to remove the skin covering the eye. However, care has to be taken not to damage the large artery arteria occipitalis.

After having exposed the sclera in this manner, it is carefully scratched with a sharp-edged surgical scalpel (blade No. 11), until a fine black hole becomes visible in it. This is the most difficult part of the preparation: immediately adjacent to the sclera there is the 'choroid' with a thickness of about 100 μm, which ensures the blood supply to the retina, and the retina itself. An injury to these layers must be avoided by all means, because the retina is turned outwards solely by the excess pressure within the eye chamber. Even the smallest damage to these layers would lead to a pressure compensation and to a spontaneous collapse of the whole eye.

When this procedure has been carried out successfully, along the edges of the tiny hole the sclera can be lifted carefully with a pair of tweezers. In this way the small hole can be enlarged systematically. Eventually nearly the whole sclera of the upper part of the eye can be removed (see Fig. 1). Because of the sclera and the skin covering the eye only serve as mechanical protection, the optimal physiological in vivo state of the rod outer segments is not impaired by this preparation.

Apparatus

In all experiments a Kratky-camera, focus, 0.1 mm × 0.2 mm (point-focus), was used. A rotating anode generator, Rigaku Rotaflex RU 200 V, served as X-ray source. Operating conditions: high-voltage, 45 kV; tube current, 200 mA. For the measurements the radiation of the Cu-Kα line was applied with

a wave length of 0.154 nm. The scattering-intensity was registered by a linear position-sensitive proportional counter (PSP-counter, Braun & Siemens) [15]. The measured diffraction intensity was stored as an intensity position diagram by a multi-channel analyzer.

Evaluation method

The calculation of the electron density profile from the measured scattering data was done according to the procedure published by Welte and Kreutz [13]. In this procedure, an arbitrary electron density profile is varied iteratively, until the corresponding theoretical 'model intensity' is in as near as possible agreement with the experimental pattern. The formulae given by Welte and Kreutz to calculate the 'model intensity' are universally valid. For example, they also take into account the influence of undulations of the membrane surface. Because of this universality and the connected complexity, the computer procedure, developed on the basis of these formulae, in practice cannot analyze diffraction-patterns with more than six or seven diffraction-spots.

Therefore, for the analysis of the rod outer segments X-ray diffraction patterns a new, reduced version of this procedure was elaborated to meet the special conditions of the rod outer segments. Following, a brief general survey of the most essential points of this version is given.

Eight assumptions (1—8) concerning the investigated object have to be valid: 1, The object is a statistical collection of membrane stacks. The individual diffraction patterns of all these stacks are superimposed incoherently. 2, As a good approximation, each disc can be considered to be a perfectly plane vesicle. (This requirement is certainly met by the rod outer segments; the undulations of the disc membrane, which are recognizable in electron microscopic pictures, are so small that they do not have any influence on the calculation of the model intensity. This is proved by theoretical estimations [13] and by model calculations carried out with the original procedure of Welte and Kreutz [13], in which the influence of small undulations was tested). 3, The extension of a disc along the plane perpendicular to the stacking axes, i.e. the lateral extension, is large compared with the extension in the direction of the stacking axis (for the rod outer segment discs the ratio is approx. 200 : 1). 4, The orientations of all stacking axes in the examined specimen show statistical fluctuations around a main direction. 5, Each rod outer segment consists of a quasi-crystalline stack of single membranes arranged in mirror-image symmetry. 6, The distance of two single membranes of one disc ('inner distance') and the distance of two neighbouring membranes of different discs (outer distance) may show uncorrelated statistical fluctuations. 7, The electron density in the inter- and intra-disc space may differ from the mean electron density of the whole stack. 8, The number n of discs within a stack shows fluctuations around a mean value n_0; the standard deviation $\sigma(n)$ is small compared with n_0; n_0 is large compared with 1. Due to assumptions 1—3 the influence of fluctuations of the orientations (see assumption 4) can be ignored by applying the well-known Lorentz correction: after multiplying the experimental intensity $I_{exp}(b)$ by b^2 one gets an intensity pattern $I(b)$, which is equivalent to a diffraction pattern of a collection of stacks arranged in parallel. The scattering vector b signifies the distance of a

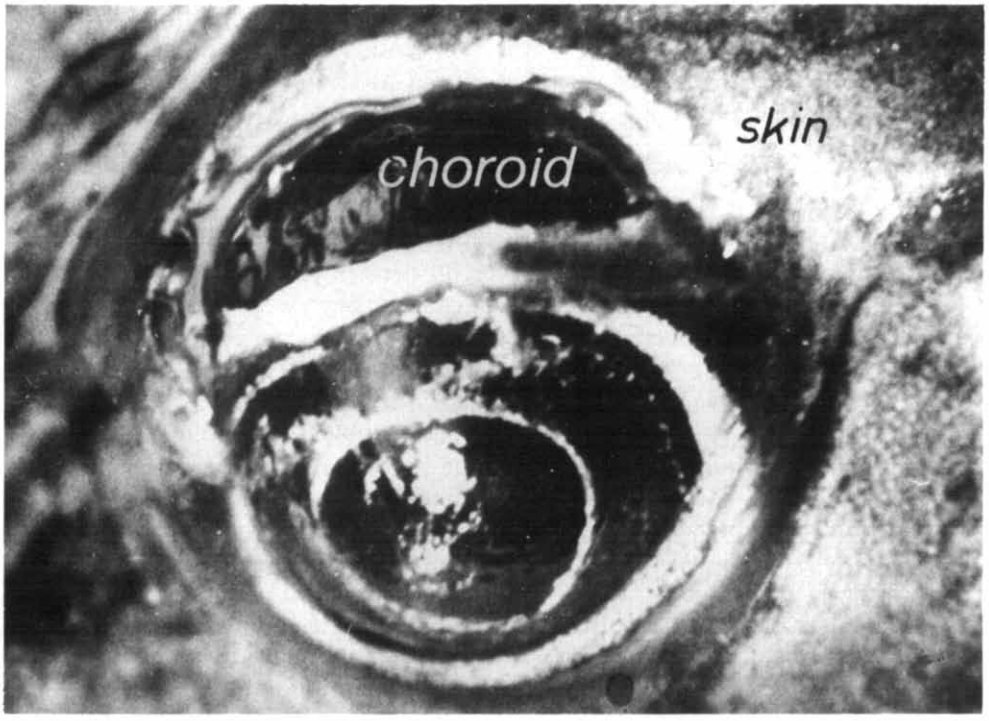

Fig. 1. Frog eye after preparation for the X-ray experiment. The skin covering the eye and the sclera are dissected. The choroid of the upper part of the eye can be seen. Immediately adjacent to the choroid there is the retina with the rod outer segments.

reflexion point from the origin of the reciprocal space, measured along the main direction of the orientations of all stacking axes. The calculation of the theoretical intensity $I(b)$ is carried out by the following steps:

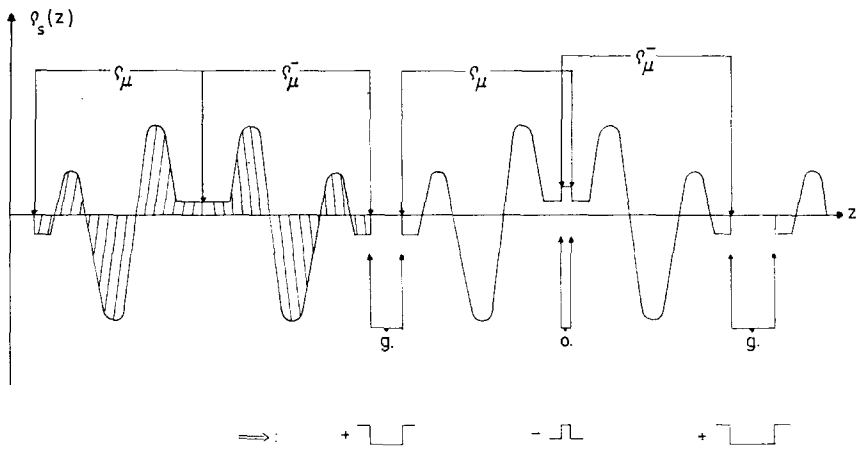

Fig. 2. Description of the electron density profile $\varrho_s(z)$ of a membrane stack by a sequence of elementary building blocks $\varrho_\mu\varrho_{\bar{\mu}}\varrho_\mu\varrho_{\bar{\mu}}\cdots$. Artificial gaps (g) and overlappings (o) and the corresponding rectangles, which have to be added or subtracted, are indicated.

1, The electron density profile $\rho_s(z)$ of single membrane stacks 's' is described mathematically by a sequence of fundamental building blocks $\rho_\mu \rho_{\bar{\mu}} \rho_\mu \rho_{\bar{\mu}} \cdots$ (according to assumption 5). ρ_μ stands for the electron density of a mean half-period, i.e. the average electron density profile of a single membrane with the adhering halves of the inter- and intra-disc spaces. $\rho_{\bar{\mu}}$ stands for the mirror image of ρ_μ. According to assumption 8 the mean electron density can be set to zero [13]. Because of the statistical distance fluctuations and owing to assumption 7, artificial 'gaps and overlappings' in the inter- and intra-disc spaces result from this way of mathematical description (Fig. 2). This must be corrected by adding or subtracting suitable rectangles.

2, From this function $\rho_s(z)$ the 'autocorrelation function'

$$Q_s(z) = \tilde{\rho}_s^2(z) = \int_{-\infty}^{\infty} \rho_s(z')\, \rho_s(z - z')\, dz'$$

is computed. After that the mean $Q(z)$ of the functions $Q_s(z)$ of all stacks s is calculated: $Q(z) = < Q_s(z) >$. In this calculation it is assumed that the distance fluctuations (see assumption 6) show statistical distributions which can be described by gaussian functions, S1 and S2, with standard deviations σ_1 and σ_2, respectively.

3, $I(b)$, the Fourier-transform of $Q(z)$, is computed. Owing to the well-known Shannon theorem [16] it is sufficient to derive an explicit formula by which one can calculate the value of $I(b)$ at discrete points b_1, called Shannon points. Using a Fourier cosine series for the analytical description of the electron density profile of a mean Bragg period ρ_0

$$\rho_0(z) = \rho_\mu\left(z + \frac{d}{4}\right) + \rho_\mu\left(-z + \frac{d}{4}\right)$$

$$= \sum_{k=1}^{N_c} c_k \cdot \cos\frac{2\pi k z}{d}$$

(Explanation: d, length of a mean Bragg period; N_c, number of required cos-coefficients) one gets the following formula to compute the value of the theoretical intensity $I(b)$ at the Shannon points $b_1 = 2l/Nd$ (N is a suitably chosen natural number complying: $Q(z) = 0$ for all z with $|z| > Nd/4$).

$$I(b_1) = n_0 \cdot |d_1|^2 + \sum_{j=1}^{n_0} (n_0 - j) \cdot 2 \cdot |d_1|^2 \cdot (H1(l) \cdot H2(l))^j$$

$$+ \sum_{j=0}^{n_0} (n_0 - j) \cdot (d_1^*)^2 \cdot H1(l) \cdot (H1(l) \cdot H2(l))^j$$

$$+ \sum_{j=0}^{n_0} (n_0 - j - 1) \cdot (d_1)^2 \cdot H2(l) \cdot (H1(l) \cdot H2(l))^j$$

$$+ \sum_{j=0}^{n_0} (n_0 - j) \cdot 2 \cdot d_1^* \cdot ZPI(l) \cdot (H1(l) \cdot H2(l))^j$$

$$+\sum_{j=0}^{n_0}(n_0-j-1)\cdot 2\cdot d_1\cdot ZPE(l)\cdot(H1(l)\cdot H2(l))^j$$

$$+\sum_{j=0}^{n_0}(n_0-j-1)\cdot 2\cdot d_1\cdot ZPI(l)\cdot H2(l)\cdot(H1(l)\cdot H2(l))^j$$

$$+\sum_{j=0}^{n_0}(n_0-j-1)\cdot 2\cdot d_1^*\cdot ZPE(l)\cdot H1(l)\cdot(H1(l)\cdot H2(l))^j$$

$$+\sum_{j=0}^{n_0}(n_0-j-2)\cdot(ZPE(l))^2\cdot H1(l)\cdot(H1(l)\cdot H2(l))^j$$

$$+\sum_{j=0}^{n_0}(n_0-j-1)\cdot(ZPI(l))^2\cdot H2(l)\cdot(H1(l)\cdot H2(l))^j$$

$$+\sum_{j=0}^{n_0}(n_0-j-1)\cdot 2\cdot ZPI(l)\cdot ZPE(l)\cdot H1(l)\cdot H2(l))^j$$

$$+1/2\cdot n_0\cdot ZQI(l)+1/2\cdot(n_0-1)\cdot ZQE(l)$$

Explanations:

$$d_1=\sum_{\substack{k=1\\k\neq 2l/N}}^{N_c} c_k\cdot(-\mathrm{i})^k\frac{2}{\pi(kN-2l)}\sin\left(\frac{\pi}{2}\left(k-\frac{2l}{N}\right)\right)+\frac{1}{N}c_{2l/N}\cdot(-i)^{2l/N}$$

d_1^* = conjugate complex of d_1

$$\left.\begin{aligned}H1(l)&=\exp\left(\frac{2\pi il}{N}\right)\cdot\exp\left(-\frac{2\pi^2l^2\sigma_1^2}{N^2d^2}\right)\\ H2(l)&=\exp\left(-\frac{2\pi il}{N}\right)\cdot\exp\left(-\frac{2\pi^2l^2\sigma_2^2}{N^2d^2}\right)\end{aligned}\right\}\text{Fourier transforms of S1 and S2}$$

$$ZPI(l)=\frac{ih_1}{2\pi l}\exp\left(-\frac{i\pi l}{N}\right)\cdot\left(1-\exp\left(-\frac{8\pi^2l^2\sigma_1^2}{N^2d^2}\right)\right)$$

$$h_1=\sum_{k=1}^{N_c}c_k$$

$$ZPE(l)=-\frac{ih_2}{2\pi l}\exp\left(-\frac{i\pi l}{N}\right)\cdot\left(1-\exp\left(-\frac{8\pi^2l^2\sigma_2^2}{N^2d^2}\right)\right)$$

$$h_2=\sum_{k=1}^{N_c}(-1)^k\cdot c_k$$

Using this formula and the least-squares-fit procedure of Marquardt [17], a computer routine was elaborated to carry out the analysis of the experi-

mental diffraction pattern. For a given set of 13 initial parameters, which describes the electron density profile (11 cos-coefficients and the two 'statistic parameters' σ_1 and σ_2), an average calculation time of 2 min was needed by a UNIVAC 1100, RZF Freiburg, to find the corresponding set of final parameters for which the theoretical model intensity shows the relatively best conformity with the experimental diffraction pattern.

Determination of the rod outer segment diffraction pattern

To allow a unique evaluation of the electron density profile from the experimental data in each experiment, four different diffraction patterns (dp1—dp4) were registered.

dp1, Diffraction intensity 'along the main direction of the lamellar scattering of the stack'. This pattern consists of a superposition of the 'real diffraction pattern $I_{exp}(b)$' with a continuous background scattering. To determine the 'real diffraction pattern $I_{exp}(b)$', needed for the evaluation, the continuous background scattering must be measured separately in addition. $I_{exp}(b)$ is the 'difference pattern': (diffraction intensity along the main direction of the lamellar scattering of the stack) minus (continuous background scattering). To prove the stability of the examined specimen in every case the diffraction intensity dp1 was registered at least two times with 10 000 s each. Because all of these 'partial patterns' were identical within the limits of measuring accuracy, they were summed up afterwards.

dp2, Background intensity. The measurement of the pure background-intensity was made possible because the rod outer segments in the living eye are strictly oriented towards the center of the pupil [11], whereas the

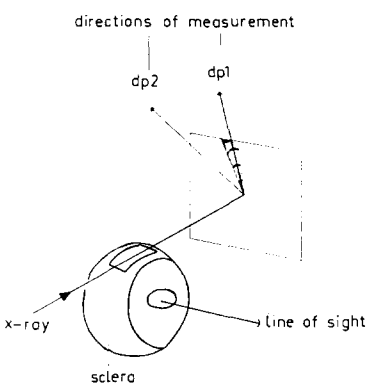

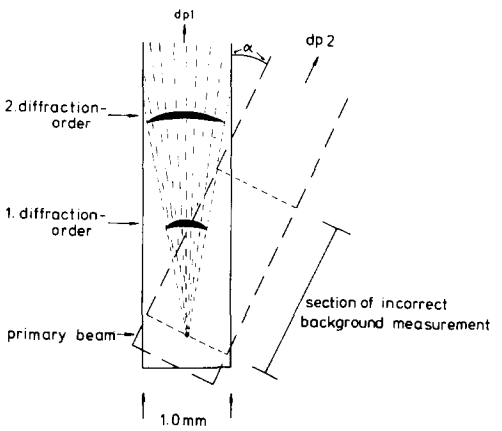

Fig. 3. Principle of the determination of the real diffraction pattern $I_{exp}(b)$. Along the main direction of the lamellar scattering the superposition of $I_{exp}(b)$ with the isotrope background scattering is measured (dp1). After rotating the counter by 25° on the axis of the primary beam the pure background scattering can be measured subsequently (dp2). Due to the strict orientation of the rod outer segments in vivo, there is no lamellar scattering beyond an angle of ±10° from the main direction.

Fig. 4. True to scale illustration of the background measurement with 1 mm counter aperture. In this case the background measurement is incorrect up to the middle of the distance 1st—2nd diffraction-order. $\alpha = 25°$.

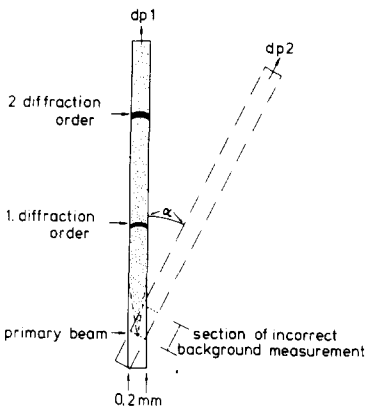

Fig. 5. True to scale illustration of the background measurement with 0.2 mm counter aperture. In this case the section of incorrect background measurement is certainly smaller than half the distance primary beam up to the 1st diffraction order. $\alpha = 25°$.

background scattering is isotropic. In order to measure the background intensity it would, therefore, be principally sufficient to rotate the PSP-counter by 25° on the axis of the primary beam after measuring the diffraction pattern dp1 (see Fig. 3). The background-scattering was also measured at least two times with 10 000 s each to study the stability of the examined specimen. Furthermore, in one case the isotropy of the background scattering was checked up by measuring also at angles of 15° and 20°.

To avoid unnecessarily long measuring times, the diffraction patterns dp1 and dp2 were registered by a PSP-counter with an aperture of 1 mm width. Due to this width, the 'difference pattern' $I_{exp}(b)$, determined in this way, is not correct within the inner section, i.e. in the section between the primary beam and the 1st diffraction order, because a part of the lamellar scattering of the stack is thus registered again while measuring the background-scattering (see Fig. 4). However, the information regarding the real course of the 'difference pattern' $I_{exp}(b)$ in the inner section is of great importance for the uniqueness of the evaluation. On account of this, the following diffraction patterns were registered in addition:

dp3, Diffraction-intensity along the main direction of the lamellar scattering of the stacks, analogous to dp1, but with a considerably reduced aperture of the counter (aperture 0.2 mm).

dp4, Background scattering, analogous to dp2, again with a considerably reduced counter-aperture (0.2 mm).

The information about the real course of the difference pattern in the inner section, which one can derive from the diffraction patterns dp3 and dp4 are sufficient for a unique determination (see Fig. 5).

Results

Diffraction patterns

Fig. 6 shows two consecutive measurements of a diffraction pattern, type dp1 (diffraction intensity along the main direction of the lamellar scattering

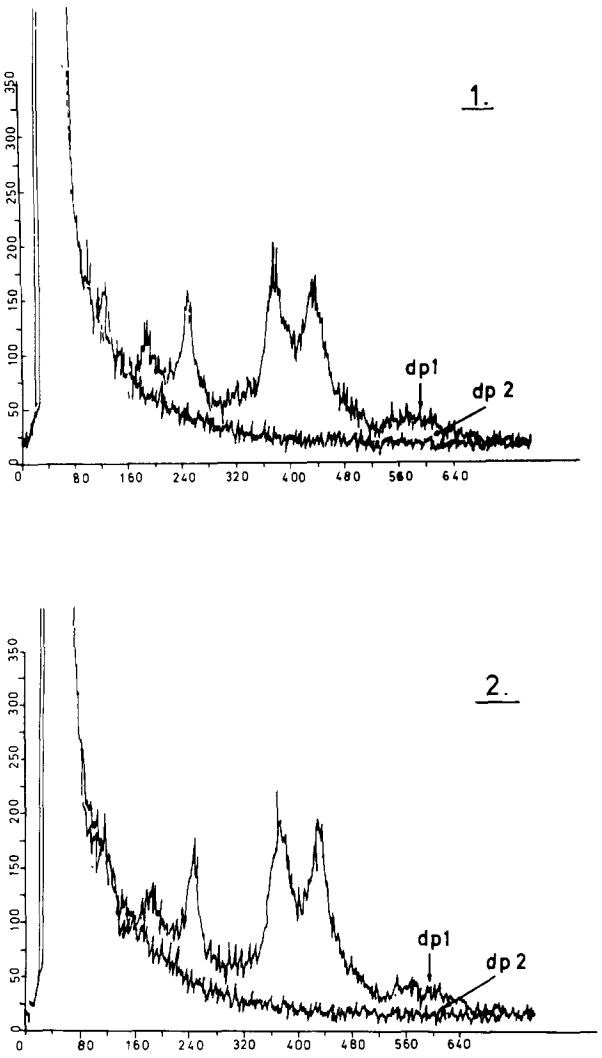

Fig. 6. Proof of stability of the examined specimen during the whole measurement. 1, First part (0—10 000 s) of the measurement along the main direction of the lamellar scattering (dp1, upper curve) together with the first part of the background scattering (dp2, lower curve). Abscissa, channel number of the multi-channel analyzer; ordinate, number of pulses registered by the counter. 2, Second part (10 001—20 000 s) of dp1 together with the second part (10 001—20 000 s) of dp2. Abscissa, channel number; ordinate, number of pulses.

of the stack) together with two corresponding measurements of a diffraction pattern, type dp2 (background-intensity). The presented patterns demonstrate that the scattering of the specimen was absolutely stable during the measurements. This fact can be regarded as an additional proof of the intact state of the examined rod outer segments.

Fig. 7 shows a representative example of complete diffraction patterns: type dp1 and dp2, respectively. To demonstrate the course of the pattern in the region of the first diffraction-order, the patterns are plotted once again,

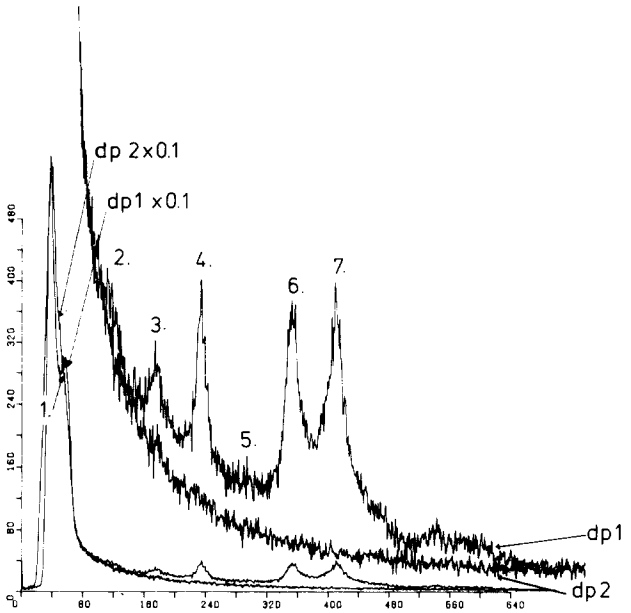

Fig. 7. Complete diffraction patterns dp1 (upper curve) and dp2 (lower curve). Abscissa, channel number; ordinate, number of pulses. Technical data of this measurement, Bragg-period = 31.6 nm; counter-aperture = 1 mm; distance specimen to counter = 275 mm; calibration of the multi-channel analyzer: 1 mm distance corresponds to 44 channels; size of primary beam = 100—200 μm.

reduced at a scale 1 : 10. In this figure one can recognize the above-described measuring artefact in the region of the first diffraction spot.

The following data are reproducible in all experiments and of great signficance for the evaluation of: 1, The sharp peaks of the 3rd, 4th, 6th and 7th

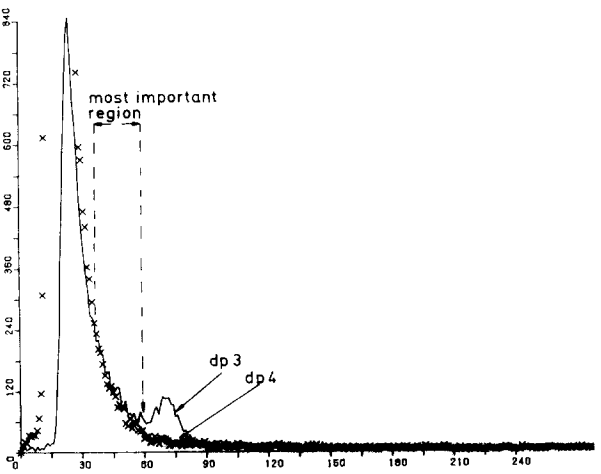

Fig. 8. Determination of the correct course of the experimental difference-pattern $I_{exp}(b)$ in the inner section. Upper curve, diffraction pattern along the main direction of the lamellar scattering (dp3); lower curve, background scattering (dp4). Counter aperture, 0.2 mm; exposure time, 3000 s; abscissa, channel number; ordinate, number of pulses.

diffraction orders in the diffraction pattern dp1 (corresponding Bragg distances: 1/10.5, 1/7.9, 1/5.3, 1/4.5; 1/nm). 2, The non-vanishing of the difference between dp1 and dp2 in the region between the 3rd and 4th as well as between the 4th, 5th, and 6th diffraction order.

Fig. 8 presents the result of a measurement of the diffraction-patterns dp3 and dp4. For the evaluation, the most essential statement of this measurement can be summed up as follows: from approximately channel No. 35 up to the origin of the first diffraction order at channel No. 58 the correct difference pattern $I_{exp}(b)$ is equal to zero.

Determination of the solution

The greatest difficulty in ascertaining the electron density profile on the basis of the experimental diffraction patterns is given by the well-known 'phase-choice problem': to each set of signs of the cosine coefficients, i.e. to each phase-choice, by which the electron density profile is described, a theoretical intensity pattern belongs which is in relatively best agreement with the experimental pattern and which can be defined as 'local solution'. One of these local solutions must be the 'global solution', representing the really true electron density profile. This global solution can only be found via computing and a comparison of all local solutions.

As the experimental difference pattern converges to 0 only beyond the 11th diffraction-order, the electron density profile of the rod outer segment disc membrane has to be described by at least 11 cosine coefficients. This would mean, that $2^{11} = 2048$ 'local solutions' have to be computed by the computer-procedure mentioned above. Because of the enormous expenditure of calculation time this is practically impossible, especially since all 2048 'local solutions' would have to be computed more than once when several experimental patterns are investigated.

In a first step this high number of local solutions can be reduced by reason of symmetry [13] to $2^9 = 512$. A second chance, certainly the most important, to reduce the number of 'local solutions' which actually have to be computed, is given by the correct measurement of the diffraction pattern $I_{exp}(b)$ in the inner section (see Fig. 8).

A brief substantiation of this criterion is given in the following: As a good approximation, the course of the theoretical intensity pattern in the inner section can be considered to be proportional to $(h_1^2 + h_2^2)$ (see Evaluation method). On the other hand, analogous to crystallographic methods, the moduli of the cosine coefficients representing the electron density can be estimated by measuring the area under the diffraction spots of the Lorentz corrected experimental difference pattern $I_{exp}(b)$. Thus, for each phase-choice the value of $(h_1^2 + h_2^2)$ can be estimated approximately without using the computer procedure.

Experience in evaluating the rod outer segment diffraction pattern has shown that there is a highest value S for $(h_1^2 + h_2^2)$. If $(h_1^2 + h_2^2)$ becomes greater than S, the corresponding theoretical intensity presents a very fast and steep increase immediately on the left of the first diffraction order (see Fig. 11). However, the exact measurement of the difference pattern $I_{exp}(b)$ in the inner section shows that this behaviour contradicts experimental facts.

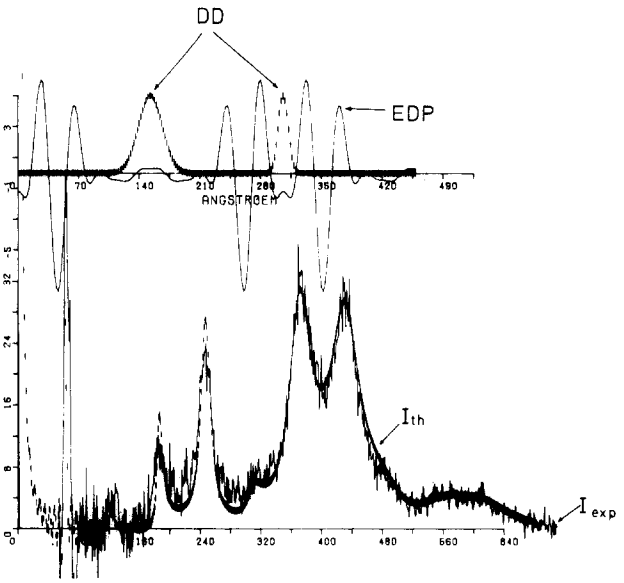

Fig. 9. Local solution with good agreement between theoretical and experimental intensity $I_{exp}(b)$. Upper coordinate system: ———, electron density profile (EDP) of three consecutive half periods; | | | | | | distance distribution (DD). Lower coordinate system; ———, $I_{exp}(b)$; | | | | | | Lorentz-corrected theoretical intensity Ith ($I(b)/b^2$). Phase choice: ++++————++++. The electron density profile is presented on an arbitrary scale, the mean electron density is set to zero.

Even if possible errors of estimation are generously taken into account, phase-choices with a value of $(h_1^2 + h_2^2)$ which exceeds the highest value S by more than 50% cannot be suitable to represent the global solution.

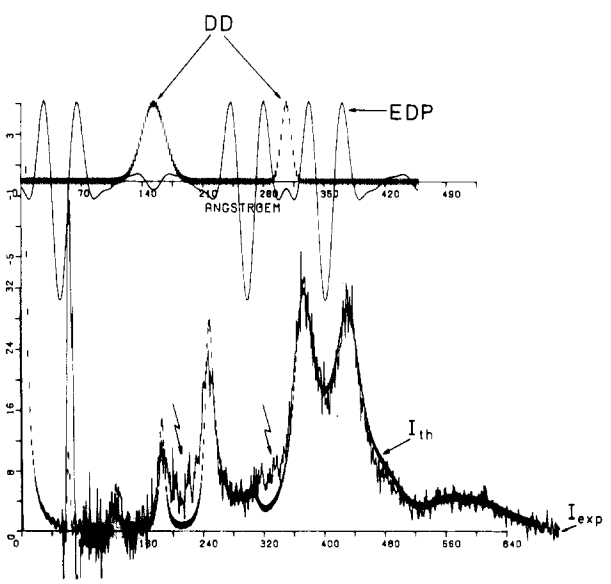

Fig. 10. Local solution with less good agreement between theoretical and experimental intensity $I_{exp}(b)$. Phase-choise: ++—+——+——+—. Places of missing agreement between theoretical and experimental intensity are indicated by ↘. For further explanations see lengend to Fig. 9.

The main measuring result of the diffraction pattern dp3 and dp4, i.e. the vanishing of the difference pattern $I_{exp}(b)$ on the left of the first diffraction order approximately up to the middle of the distance: first diffraction order up to the primary beam, requires a very low value for S.

Example (computed with the realistic coefficients $c_1 = 1.5$, $c_2 = 3.2$, $c_3 = 6.2$, $c_4 = 15.9$, $c_5 = 12.9$, $c_6 = 40.7$, $c_7 = 47.6$, $c_8 = 8.9$, $c_9 = 22.9$, $c_{10} = 34.3$, $c_{11} = 2.5$):

Phase-choice ++++++++++ : $h_1^2 + h_2^2 = 38\,777$.

Phase-choice +++++|− − − +++ : $h_1^2 + h_2^2 =$ 35.

Highest value S (empirical value) = 1400.

In this way, the number of local solutions which actually had to be computed could be reduced from 512 to about 59! Among these 59 phase-choices there were only four, i.e. the sets ++++− − −+++, +++− −+−++−+, ++− −++++− − − and ++−++−+− −+−, which show a sufficiently good agreement of their corresponding theoretical intensities with the experimental difference pattern. One representative example of these remaining four phase-choices is presented in Fig. 9.

All of the other 55 phase-choices led to theoretical intensity patterns which showed decisive discrepancies as to the experimental pattern, for example as shown in Fig. 10; these, therefore, could be excluded from representing the global solution. A further restriction to only one single possible phase-choice was not practicable after that. Fortunately, this restriction was not at all necessary, because the electron density profiles, represented by the remaining four possible phase-choices, were not distinguishable among one another within the limits of the available resolution. (The fact that the different phase-choices lead to non-distinguishable electron density profiles can be easily explained, because a change in the sign of the very small coefficients c_1 and c_2 can be compensated by slightly modifying the large coefficients.) The electron density profile presented in Fig. 9 must therefore represent the global solution.

Discussion

The analysis of X-ray diffraction patterns of paracrystalline membrane stacks alone does not permit a definite answer to the question: which one of the spaces is the inter- and which one is the intra-disc space, i.e. in which space does the center of symmetry of the disc lie. Furthermore, for each solution also its mirror-image relating to the abscissa yields another solution of the same quality. Nevertheless, a unique interpretation, particularly of the results presented here, is possible, since only one of the possible interpretations is not in contradiction to the generally accepted facts (see Introduction) that: 1, the inter-disc space is obviously larger than the intra-disc space (this fact is confirmed by a large number of electron-microscopic pictures [18—20]); 2, the basic structure of the disc-membrane is a lipid-bilayer.

This single possible explanation of the electron density profile of the rod outer segment disc membrane in vivo is presented in Fig. 12. An important

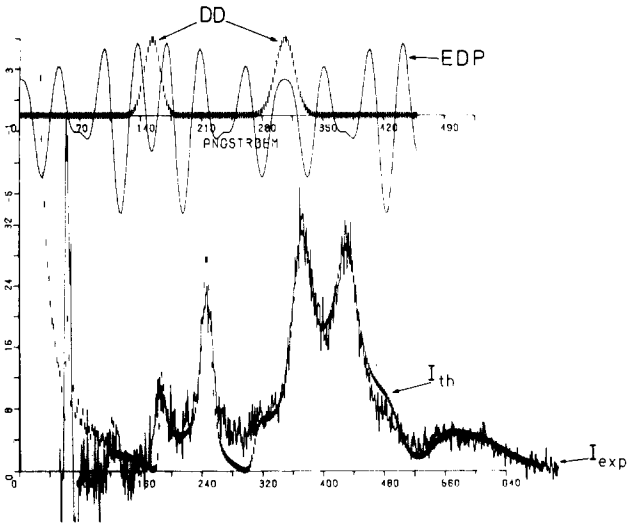

Fig. 11. Local solution with bad agreement between theoretical and experimental intensity $I_{exp}(b)$. Phase choice: ++++++−−−−−+. Especially the course of the theoretical intensity pattern immediately to the left of the first diffraction order is in contradiction to the experimental results. For further explanations see Legend to Fig. 9.

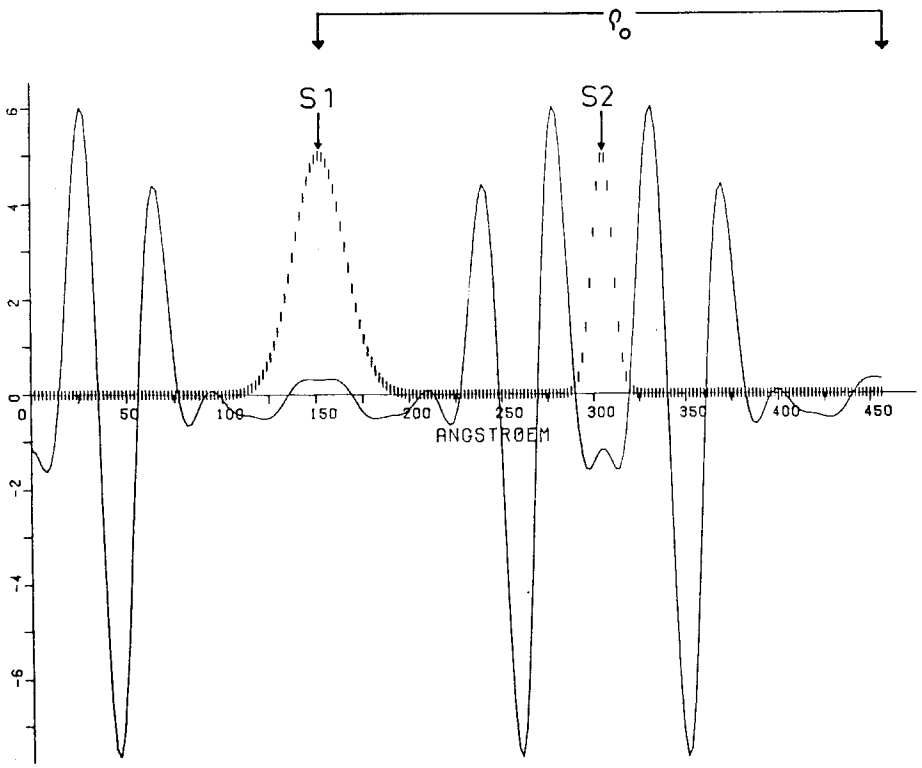

Fig. 12. Electron density profile of the rod outer segment discmembrane in vivo. ρ_0, electron density profile of one disc with the adhering halfs of the inter-disc-spaces; S1, statistical distribution of the fluctuations of the outer distance; S2, statistical distribution of the fluctuations of the inner distance. The electron density profile is presented on an arbitrary scale. The mean electron density is set to zero.

result of our examinations is contained in the ascertainment that the electron density in the head-group region of the side of the membrane which is in contact with the cytoplasm ('outer face') is clearly lower than the electron density in the head-group region of the side which is in contact with the disc lumen ('inner face'). Judging from the literature, for example of Krebs and Kühn [21] who report that rhodopsin amounts to a share of about 95% of the whole mass of all disc proteins, one cannot but conclude that the main portion of the mass of rhodopsin is concentrated near the inner face of the membrane.

Other authors [22] state that the share of rhodopsin among the whole mass of the disc proteins is only 55%. According to these assumptions a unique statement about the mass distribution of rhodopsin only on the basis of the electron density profile is not possible, because other proteins and perhaps a small asymmetry of the basic structure of the lipid bilayer could overcompensate the form of this mass distribution. In any case, it can be ruled out that rhodopsin and other high-molecular proteins are concentrated mainly on the cytoplasmic side of the membrane.

Moreover, the determined electron density profile allows two additional conclusions: 1, within the disc lumen the electron density is certainly lower than within the cytoplasm; 2, Every two neighbouring discs cannot get closer than about 7 nm. (This can be concluded from the relatively narrow distance distribution in the inter-disc space.)

A comparison of studies on the electron density profile published up to the present must be interpreted very carefully alone for the reason that in the literature there are no electron density profiles evaluated on the basis of experiments carried out with living animals. Nevertheless, particularly a comparison of the papers published more recently by Chabre [6] on the one hand an by Dratz and co-workers [8,9] on the other is of great interest. In these papers the background scattering is apparently determined by 'measuring by eye', i.e. a background scattering is proposed which appears to be suggestive with respect to the lamellar diffraction pattern.

In Chabre's paper [6] this background intensity is chosen in such a manner that the difference pattern $I_{exp}(b)$ is equal to zero in the region between the 3rd and the 4th diffraction orders. The corresponding electron density profile presents a slightly asymmetric bilayer with a higher electron density on the cytoplasmic edge of the membrane than on the side in contact with the disc lumen.

In the papers of Dratz and co-workers [8,9], on the other hand, the background-scattering is chosen in such a manner that the difference pattern is clearly unequal to zero in the region between the 3rd and the 4th diffraction orders (see Ref. 8). The evaluated electron density profile presents an asymmetric bilayer with a higher electron density near the inner face of the disc membrane than near the outer face.

Electron density profiles which were similar in quality to one of each of these two profiles appeared as local solutions also in our investigations (see Figs. 9 and 10). The local solution presented in Fig. 10 could, however, be excluded from representing the global solution, because the agreement of its theoretical intensity pattern with the experimental pattern was not good enough.

The main reason for this disagreement was that the experimental difference pattern $I_{exp}(b)$ clearly differs from zero in the region between the 3rd and 4th diffraction orders, whereas the theoretical intensity pattern of this local solution is equal to zero in that region. This rejected local solution comes close to the solution given by Chabre [6].

Conversely, the choice of the background-intensity in the papers of Dratz and coworkers [8,9] is in better agreement with results determined by our experiments. Consequently, the electron density profile evaluated by them possesses considerably more analogies to the profile determined in our investigation.

Acknowledgement

We are especially grateful to Mr. D. Walter for his assistance with the registration of the X-ray patterns, to Mrs. G. Heppeler who introduced us to the treatment of frogs, and to Mrs. W. Herbst for her help in preparing the English version of the paper.

References

1 Hofmann, K.P., Uhl, R., Hofmann, W. and Kreutz, W. (1976) Biophys. Struct. Mech. 2, 61—77
2 Uhl, R., Hofmann, K.P. and Kreutz, W. (1977) Biochim. Biophys. Acta 469, 113—122
3 Blaurock, A.E. and Wilkins, M.H.F. (1969) Nature 223, 906—909
4 Blaurock, A.E. and Wilkins, M.H.F. (1972) Nature 236, 313—314
5 Worthington, C.R. (1974) J. Gen. Physiol. 62, 53—86
6 Chabre, M. (1975) Biochim. Biophys. Acta 382, 322—335
7 Chabre, M. and Cavaggioni, A. (1973) Nature New Biol. 244, 118—120
8 Schwartz, S., Cain, J.E., Dratz, E.A., Blasie, J.K. (1975) Biophys. J. 15, 1201—1233
9 Dratz, E.A., Miljanich, G.P., Nemes, P.P., Gaw, J.E. and Schwartz, S. (1978) Photochem. Photobiol. 29, 661—670
10 Webb, N.G. (1972) Nature 235, 44—46
11 Webb, N.G. (1977) Vis. Res. 17, 625—631
12 Webb, N.G. (1972) X-Ray Diffraction Studies of Retinal Rod Outer Segment and Related Membranes, Thesis, Kings College, London
13 Welte, W. and Kreutz, W. (1979) Adv. Polymer Sci. 30, 163—225
14 Funk, J., Wutschel, I., Welte, W. and Kreutz, W. (1979) Annual Meeting of the Deutsche Gesellschaft für Biophysik, Springer Verlag, Berlin
15 Broll, N., Henne, M. and Kreutz, W. (1979) Siemens Analysentechnische Mitteilung Nr. 271, Int. Edn.
16 Papoulis, A. (1968) Probability, Random Variables and Stochastic Processes, MacGraw Hill, New York
17 Marquardt, D.W. (1963) J. Soc. Indust. Appl. Math. 2, 431—441
18 Rodieck, R.W. (1973) The Vertebrate Retina, Freeman, San Francisco
19 Nilsson, S.E.G. (1965) J. Ultrastruct. Res. 12, 207—231
20 Sjöstrand, F.S. and Kreman, M. (1978) J. Ultrastruct. Res. 65, 195—226
21 Krebs, W. and Kühn, H. (1977) Exp. Eye Res. 25, 511—526
22 Siebert, F., Schmid, H. and Mull, R.H. (1977) Biochem. Biophys. Res. Commun. 75, 1071—1077